

valuable discussions, suggestions, and criticisms during the writing of this paper. Thanks are due to the members of the Plasma Physics Laboratory of Princeton University for valuable discussions. It gives me great pleasure to point out that my knowledge of the basic physical principles used in this paper were gained from

the lectures of Professor F. Villars, Professor F. E. Low, Professor S. C. Brown, and Professor K. Huang of M.I.T.

This work was performed under the auspices of the U. S. Atomic Energy Commission, Contract No. AT(30-1)-1238.

PHYSICAL REVIEW

VOLUME 149, NUMBER 1

9 SEPTEMBER 1966

Stimulated Brillouin Scattering in Liquids*

ALAN S. PINE

Gordon McKay Laboratory, Harvard University, Cambridge, Massachusetts

(Received 8 April 1966)

Stimulated Brillouin scattering in various liquids is examined in a transverse resonator and in a backward-wave oscillator. Comparison with elementary resonator theory indicates that the data are in satisfactory agreement for many liquids. The theoretical picture for the unstable backward-wave configuration is complicated by phonon transit-time effects, but even here the results establish guidelines for the theory. It is found necessary to discard the results for some liquids because of self-focusing and other nonlinear processes which interfere with the Brillouin effect.

I. INTRODUCTION

SOME experiments on stimulated Brillouin scattering in liquids are devised to test the validity of existing theories on the subject. The use of a resonator transverse to a laser beam provides the most direct confirmation of the quantum theory of Yariv¹ and Pine² or the equivalent classical theory of Chiao.³ Threshold behavior of the more conventional backward-wave configuration is examined but does not yield conclusive proof of either the theory of Kroll⁴ or Bloembergen.⁵ It does, however, indicate the parameters of importance for any such theory.

Based on measurements of observational thresholds for 180° and 90° scattering and of total output in the transverse resonator, the liquids divide into two classes coincident with the previously distinguished⁶ non-self-focusing (NSF) and self-focusing (SF) categories. The NSF liquids behave in stimulated Brillouin scattering as would be expected from their photoelastic properties. Self-focusing liquids however correlate poorly with hypersonic parameters as many parasitic effects are in evidence.

* This work was supported by the Office of Naval Research.

¹ A. Yariv, *J. Quant. Electron.* **1**, 41 (1965).

² A. Pine, thesis, and College of Engineering, University of California, Berkeley, ERL Technical Memorandum M-117, 1965 (unpublished).

³ R. Chiao, thesis, Massachusetts Institute of Technology, 1965 (unpublished).

⁴ N. Kroll, *J. Appl. Phys.* **36**, 34 (1965).

⁵ N. Bloembergen, *Nonlinear Optics* (W. J. Benjamin, Inc., New York, 1965).

⁶ N. Bloembergen, P. Lallemand, and A. Pine, in Proceedings of the Conference of Quantum Electronics, Phoenix, Arizona, 1966 (unpublished); *J. Quant. Electron.* (to be published).

Spectral output, radiation patterns, and temporal behavior identify the Brillouin effect. Other competitive nonlinear effects are disclosed by these measurements and by study of concomitant Raman radiation.

II. EXPERIMENTAL RESULTS

The apparatus of the transverse-resonator experiment is depicted in Fig. 1. It is similar in nature to that used by Dennis and Tannenwald⁷ to study the Raman effect and by Dennis⁸ to obtain Brillouin radiation. Takuma and Jennings⁹ used an off-axis cavity at small angles to study the Brillouin effect. These latter two experiments were performed with a limited range of liquids and in the Dennis case with an ambiguous

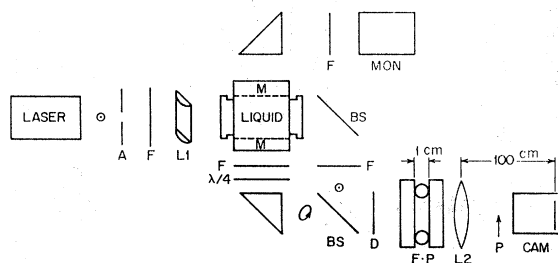


FIG. 1. Experimental schematic for stimulated scattering in a transverse resonator. A, aperture; F, filters; L, lenses; BS, beam splitters; D, diffuser; $\lambda/4$, depolarizer; F-P, interferometer; P, polarizer; M, mirrors.

⁷ J. Dennis and P. Tannenwald, *Appl. Phys. Letters* **5**, 58 (1964).

⁸ J. Dennis, Lincoln Laboratory, Solid State Research Report No. ESD-TDR-65-31, 1964 (unpublished).

⁹ H. Takuma and D. Jennings, *Appl. Phys. Letters* **5**, 239 (1964).

TABLE I. Photoelastic parameters and stimulated Brillouin outputs and thresholds for several liquids.

Liquid	Photoelastic parameters		Peak output power $P(\omega_L^{\dagger})$, (kW)		Threshold power		Threshold length for ω_B^{\parallel} , laser unfocused (cm)
	$\gamma^2/n\rho v$ (10^{-5} cgs units)	$\gamma^2/n\rho v(\Delta\nu)$ (10^{-14} cgs units)	3.7-cm cavity	5.0-cm cavity	% $P(\omega_L)$ focused 3.7-cm cavity	% $P(\omega_L)$ unfocused 1.6-cm cavity	
1. C ₆ H ₁₄	1.33	12.0	65	45	28	76	5.5±0.5
2. C ₆ H ₁₂	1.32	2.9	63	35	36	...	11±1
3. (C ₂ H ₅) ₂ O	1.15	9.7	51	...	32	74	...
4. CCl ₄	1.01	2.2	51	4	37	...	12±1
5. C ₂ H ₅ OH	0.95	5.4	43	...	43
6. C ₂ H ₆ O	0.89	7.9	38	2	35	...	6.5±0.5
7. CH ₃ OH	0.75	6.0	15	0.5	36	...	8.5±1
8. H ₂ O	0.48	3.0	0.1	0.005	88	...	33±3
9. C ₆ H ₅ CH ₃	1.70	5.8	50	7	21	98	4.6±0.1
10. C ₆ H ₆	1.56	10.6	30	2	27	85	4.6±0.1
11. C ₆ H ₅ NO ₂	1.53	...	5	0.3	27	...	1.7±0.1
12. CS ₂	1.91	73	2	0.2	10	45	1.7±0.1

Brillouin shift determination due to multimode laser excitation. A stimulated Brillouin emission at 90° was seen without a resonator in quartz by Chiao, Townes, and Stoicheff,¹⁰ but no such effect has been reported in liquids.

The laser is a cryptocyanine switched ruby, mode-selected to give a linewidth of 0.02 cm⁻¹. Maximum power, $P(\omega_L)$, is roughly 14 MW with a pulse duration of 12 nsec. The cavity is formed by two multilayer dielectric mirrors spaced by 5.0, 3.7, or 1.6 cm and reflecting >99% at 6943 Å. In the first two cavities Brillouin oscillation is seen when the laser is focused with a cylindrical lens ($f=5$ cm), but in the 1.6-cm cavity threshold could be exceeded in some liquids without focusing. Output power is monitored by an S-20 photosurface planar diode with 5-W sensitivity and 1-GHz bandwidth.

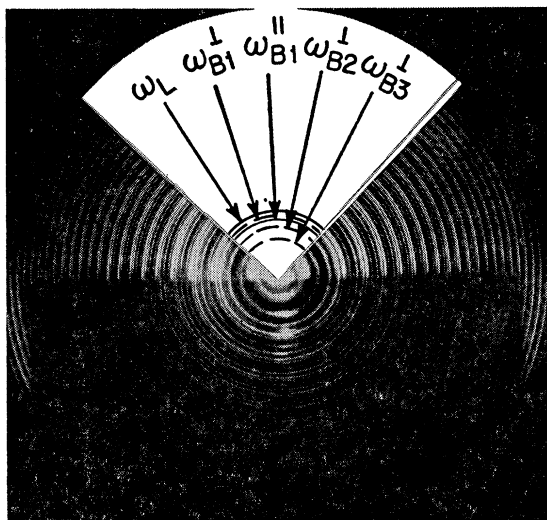


FIG. 2. Interferogram of stimulated Brillouin radiation in a transverse resonator. *n*-hexane, inter-order spacing 0.494 cm⁻¹.

¹⁰ R. Chiao, C. Townes, and B. Stoicheff, Phys. Rev. Letters 12, 592 (1964).

In the backward-wave configuration the laser is directed through a 3.6-mm aperture into a variable-length cell. Threshold lengths are observed by detecting forward Raman-Stokes radiation with 1-W sensitivity in an acceptance angle of 50 mrad and by detecting backward Brillouin scattering with 200-W sensitivity in a cone of 0.5 mrad. The cell windows are tilted ~3° to reduce feedback and reflections to the detectors.

A typical stimulated Brillouin output display of the transverse resonator is given in Fig. 2. The radiation from the resonator passes through a quarter-wave plate so that it may be distinguished from the linearly polarized laser and backward Brillouin light. The two beams are combined in a Fabry-Perot interferometer (inter-order spacing 0.494 cm⁻¹) and photographed with a polarizer blocking half the film. An unambiguous identification of the lines is possible from the frequency shifts and intensities. For *n*-hexane, the laser stimulates a 180° scattering, ω_{B1}^{\parallel} , with a splitting of 0.14 cm⁻¹ and a 90° scattering, ω_{B1}^{\perp} , with splitting 0.10 cm⁻¹. An iterative backscattering process then goes on in the cavity starting from ω_{B1}^{\perp} to ω_{B2}^{\perp} to ω_{B3}^{\perp} with frequency shifts 0.14 cm⁻¹. Further multiple orders of either ω_B^{\perp} or ω_B^{\parallel} can be generated competitively by repositioning the focus of the cylindrical lens. Also ω_{B2}^{\perp} seems not to be generated by ω_{B1}^{\parallel} since the intensity ratio $[P(\omega_{B1}^{\parallel})/P(\omega_L)]$ is much less than $[P(\omega_{B2}^{\perp})/P(\omega_{B1}^{\perp})]$.

Interestingly, no Brillouin anti-Stokes radiation is observed at $\omega_{B1}^{\perp}+0.14$ cm⁻¹ even though phonons and pump propagate antiparallel in the cavity. The small phase mismatch involved in the parametric generation of anti-Stokes radiation gives a coherence length² of $\pi c/2n(\omega_{B1}^{\perp}-\omega_{B2}^{\perp})$, where c/n is the velocity of light in the medium. Typically this is 1 to 2 cm, which is slightly smaller than the cavity liquid column.

The data on several liquids are presented in Table I together with the pertinent acoustical properties of the liquids. The first eight liquids are in the NSF category while the remainder are SF liquids. Output powers are

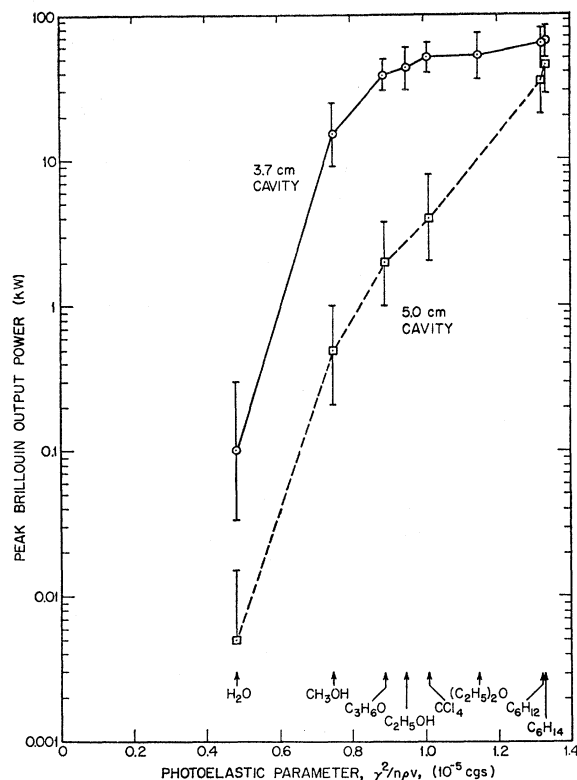


FIG. 3. Transverse resonator Brillouin conversion efficiency for non-self-focusing liquids.

the peak powers from the 90° resonator, threshold power refers to the input (focused for the 3.7-cm cavity, unfocused for the 1.6-cm cavity) for which the stimulated radiation drops below detection sensitivity, threshold length corresponds to observability of Brillouin radiation in the backward-wave configuration with the laser not prefocused. n , ρ , and v are the refractive index, density, and sound velocity of the liquids; γ is the electrostrictive coupling parameter taken to be the phenomenological $(n^2-1)(n^2+2)/3$ from the Lorenz-Lorentz law; $\Delta\nu$ is the acoustic linewidth. The velocity and linewidths are interpolated from the data of Chiao and Fleury¹¹ obtained by normal Brillouin scattering and from supplementary data obtained by the author using similar techniques.

III. THEORETICAL RESUMÉ AND COMPARISON WITH EXPERIMENT

In a resonator the amplitude gain at time t after turning on the pump is $\exp\delta t$, where the eigenvalues

$$\delta_{\pm} = \frac{1}{2}(\Gamma_c + \Gamma_v) \pm \left\{ \frac{1}{4}(\Gamma_c - \Gamma_v)^2 + \epsilon^2 \right\}^{1/2}. \quad (1)$$

Here the damping constants are related to the decay time in the optical cavity τ_{oc} , and the acoustic linewidth

¹¹ R. Chiao and P. Fleury, in *Physics of Quantum Electronics*, edited by P. Kelley, B. Lax, and P. Tannenwald (McGraw-Hill Book Company, New York, 1966), p. 241.

by

$$\Gamma_c = (2\tau_{oc})^{-1}; \quad \Gamma_v = 2\pi(\Delta\nu), \quad (2)$$

and

$$\epsilon^2 = (\gamma^2/n\rho v)(I_L k_L^2)^{1/8} \sin(\theta/2). \quad (3)$$

I_L and k_L are the incident laser intensity and wave vector; $\sin(\theta/2)$ is the Bragg factor involving the scattering angle θ . This is the result of a linearized parametric theory of stimulated Brillouin emission²; it does not include pump saturation or multiple scatterings.

In the heavily damped regime where $\Gamma_v \gg \Gamma_c$ or 2ϵ , the light-like eigenmode has positive gain when

$$\delta_+ \approx -\Gamma_c + \epsilon^2/\Gamma_v > 0. \quad (4)$$

The highly excited regime where $2\epsilon \gg \Gamma_v$ or Γ_c is characterized by a mixed mode with gain

$$\delta_+ \approx \epsilon. \quad (5)$$

The crossover intensity, for which $2\epsilon = \Gamma_v$, is 10–100 MW/cm² for most liquids.

The highly excited domain is attained in this experiment at full-focused laser power. Experimentally the gain may be enough to saturate the pump and one must speak of a "conversion efficiency" rather than a parametric gain. The efficiency is measured by the peak powers in Table I and it is seen to order according to $\gamma^2/n\rho v$ (or ϵ) rather than to $\gamma^2/n\rho v(\Delta\nu)$ (or ϵ^2/Γ_v)—at least for NSF liquids. A replot of these data in Fig. 3 demonstrates this correlation and gives a clearer indication of the saturation phenomenon and the fluctuations in the data.

Threshold power in the 3.7-cm resonator does not agree exactly with the highly excited or the heavily

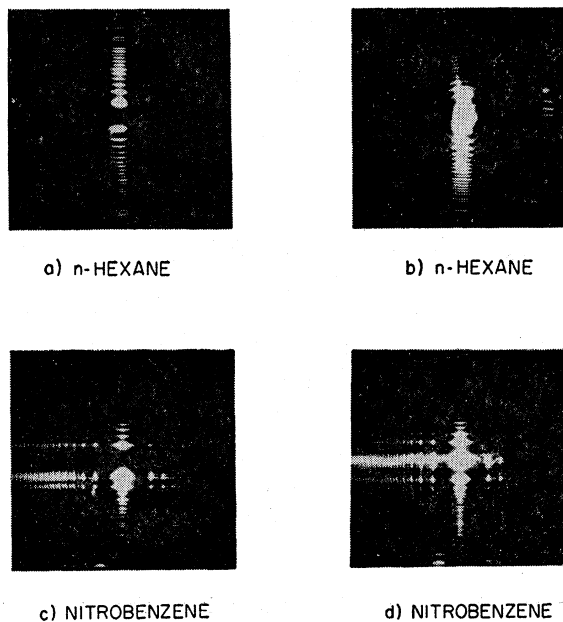


FIG. 4. Far-field patterns of Brillouin radiation from a 5.0-cm resonator.

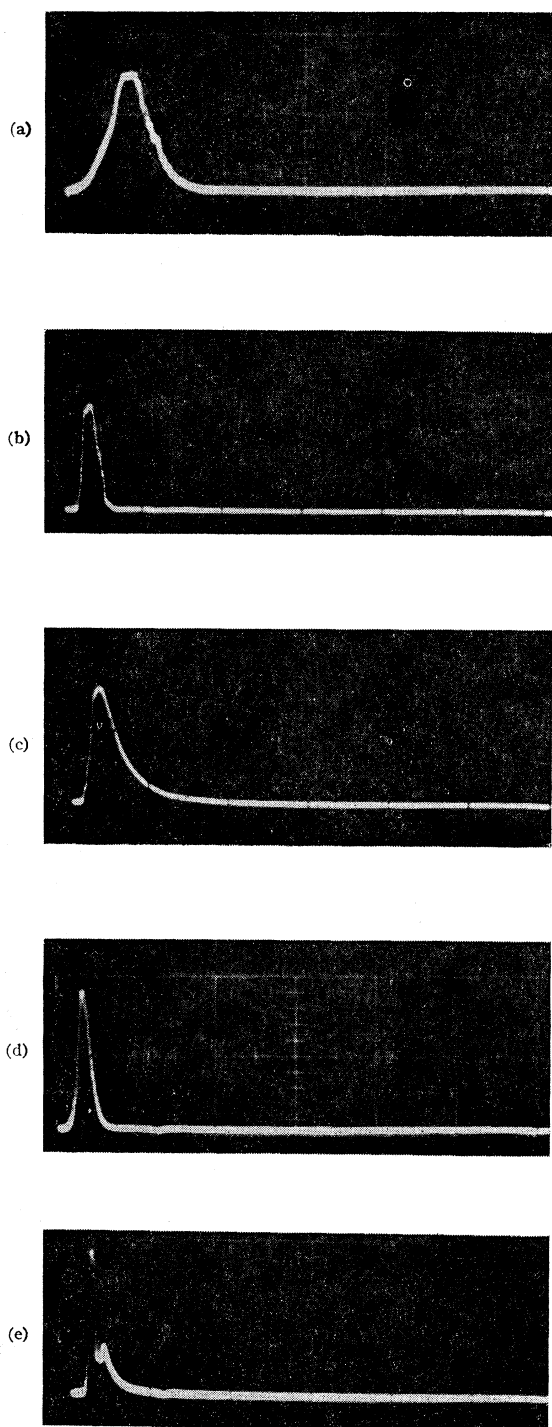


FIG. 5. Time-resolved stimulated Brillouin emission 20 nsec/div.; 1-GHz bandwidth. (a) Laser, ω_L ; (b) Brillouin at 180° in 12-cm cell of *n*-hexane with laser unfocused; (c) Brillouin at 90° in *n*-hexane; (d) Brillouin at 90° in nitrobenzene; (e) Brillouin at 90° in cyclohexane.

damped theory. This is not surprising since the gain required for the observational threshold far exceeds the minimal gain condition of Eq. (4). Furthermore, the

laser beam fills only 10 to 20% of the transverse cavity so that the effective time for gain is a factor 5 to 10 less than the pulse duration. This gain must then be balanced against the optical-cavity loss for the entire pulse length to obtain a true threshold condition. In spite of these difficulties a trend toward the heavily damped regime is manifest in the relatively high thresholds of the lossy liquids, CCl_4 and C_6H_{12} , and the low threshold of CS_2 —all out of order with conversion efficiency measurements.

For the unfocused laser in the 1.6-cm cavity the results indicate the strong influence of damping even though, theoretically, intensities are in the crossover region. The data here are too sparse to draw definite conclusions. In addition the SF liquids create further interpretational difficulties as will be seen in the following section.

Where data are available for NSF liquids, it is observed that the heavily-damped-resonator theory correlates well with the observational threshold lengths for backscattering in a collimated laser. The same acoustic parameters are involved, of course, in the traveling wave theories. Whether the steady-state theory of Bloembergen or the mixed space-time considerations of Kroll apply to this case cannot be determined. However, it is certain that acoustic damping—and not electrostrictive self-focusing¹²—dominates the backward-wave Brillouin effect. Brewer's¹³ findings in *n*-hexane, which appear to support Kroll's theory, may be interpreted otherwise if one allows for a finite development time of the instability and the poor sensitivity of threshold detection.

As has been reported previously,⁶ the threshold lengths in SF liquids for the backward Brillouin effect appear to arise from Kerr-effect self-focusing. Aside from a good correlation with the optical molecular anisotropy, one has the additional evidences of simultaneous Brillouin-Raman thresholds, filament formation, and frequency broadenings. The NSF liquids, to the contrary, show a much higher Raman than Brillouin threshold and little tendency to form filaments or broaden frequencies.

IV. EXPERIMENTAL COMPLICATIONS

Of the several experimental complications in the transverse Brillouin resonator, three are most noteworthy: (1) cavity-pulling effects, (2) cavity deterioration due to self-focusing, and (3) competitive Raman effect. Since the inter-order spacing of the resonator modes ($\sim 0.1 \text{ cm}^{-1}$) is larger than the combined laser and acoustic linewidths, in general the Brillouin effect does not oscillate in an on-axis mode. Because of thermal variations, the cavity spacing and laser frequency could not be controlled precisely enough to

¹² R. Chiao, E. Garmire, and C. Townes, *Phys. Rev. Letters* **13**, 479 (1964).

¹³ R. G. Brewer, *Phys. Rev.* **140**, A800 (1965).

effect exact tuning. Hence the Brillouin light tends to chose the lower Q off-axis or "walkoff" modes of the resonator. Aside from small shot-to-shot laser power variations, this tuning problem causes most of the fluctuations seen in the data of Fig. 3. Typical far-field patterns of the 5.0-cm resonator in Fig. 4 for two consecutive firings in *n*-hexane and nitrobenzene illustrate the large number of walkoff modes excited even when on-axis modes are present. The smearing of the far-field pattern in nitrobenzene is characteristic of only the SF liquids and is thought to be due to the Kerr-effect index change induced by the incident laser.

Further confirmation of Q deterioration due to the three complications listed above is presented in Fig. 5, the time-resolved radiations. For reference the laser pulse and the nonresonator backward Brillouin radiation in 12 cm of *n*-hexane are given in 5(a) and 5(b). The on-axis mode of the transverse resonator with $>1\%$ transmitting mirrors should give a decay time of >20 nsec. In *n*-hexane the off-axis modes reduce this to ~ 10 nsec; in nitrobenzene the optical inhomogeneities cause a 2-nsec decay; and in cyclohexane conversion of Brillouin to Raman radiation catastrophically decays the Brillouin output.

In the 90° cavity stimulated Raman radiation can be excited by the laser or by the 90° Brillouin light. C_6H_{12} and CCl_4 both exhibit the latter behavior as evidenced by the spiked temporal behavior as in Fig. 5(e). For this reason peak, rather than average, $P(\omega_B^1)$ is compared with theory. Two other facts attest to the validity of the Brillouin pumping scheme. Firstly Raman-anti-Stokes emission occurs at a small angle to the mirror normal (25 ± 5 mrad for the 801-cm^{-1} vibration in cyclohexane) directly involving ω_{B1} —if not as a Stokes pump, at least as a parametric source. Secondly copious Raman-Stokes emission is produced

at the 2853 cm^{-1} shifted frequency, ω_R^1 . Exchange of one of these mirrors for a reflectivity of 30% at ω_B^1 and 99% at ω_R^1 yields no stimulated effect whatsoever. If the laser directly pumps ω_R^1 , threshold would be reduced for this configuration. With two mirrors peaked at ω_R^1 and down at ω_B^1 , threshold could be exceeded on the Raman line with no Brillouin stimulation. Coincident Brillouin-Raman radiation is produced in CS_2 , toluene, and benzene, but not in nitrobenzene, with full laser power and mirrors peaked at ruby and down to 93% at 7660 \AA .

V. CONCLUSIONS

It now appears possible to interpret the stimulated Brillouin effect of many materials solely in terms of their hypersonic properties. Data on these properties such as those given by Chiao and Fleury are of primary importance, but no less critical is the isolation of the Brillouin effect from other interfering nonlinear effects. Quantitative theoretical verification is hindered in this experiment by lack of detailed knowledge of the laser-beam profile, particularly when focused. The unknown noise characteristics which initiate the oscillations similarly prevent accurate numerical analysis. Further probing into the theory, especially the heavily damped regime, seems plausible by lengthening the laser pulse and optimizing resonator size and beam dimensions. The range of materials tested should be extended and more hypersonic data is invited by independent means.

ACKNOWLEDGMENT

The author wishes to thank Professor N. Bloembergen for many helpful suggestions and a critique of the manuscript.

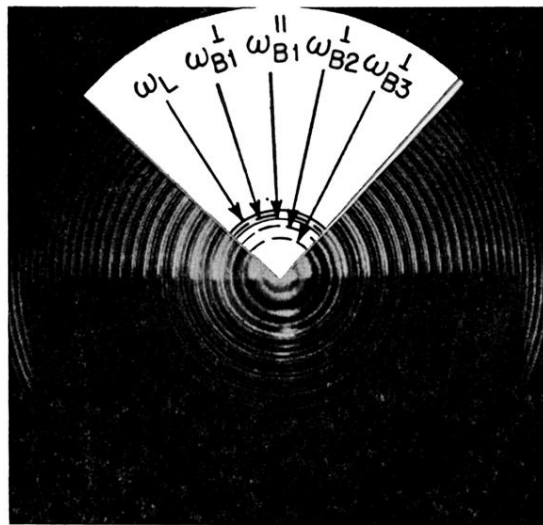
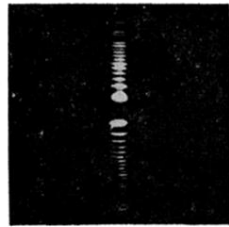
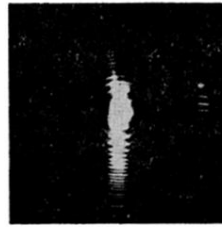


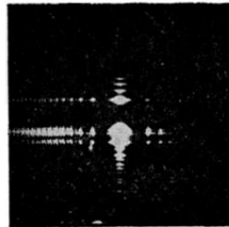
FIG. 2. Interferogram of stimulated Brillouin radiation in a transverse resonator. *n*-hexane, inter-order spacing 0.494 cm^{-1} .



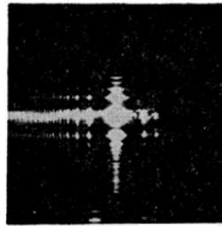
a) n-HEXANE



b) n-HEXANE



c) NITROBENZENE



d) NITROBENZENE

FIG. 4. Far-field patterns of Brillouin radiation from a 5.0-cm resonator.

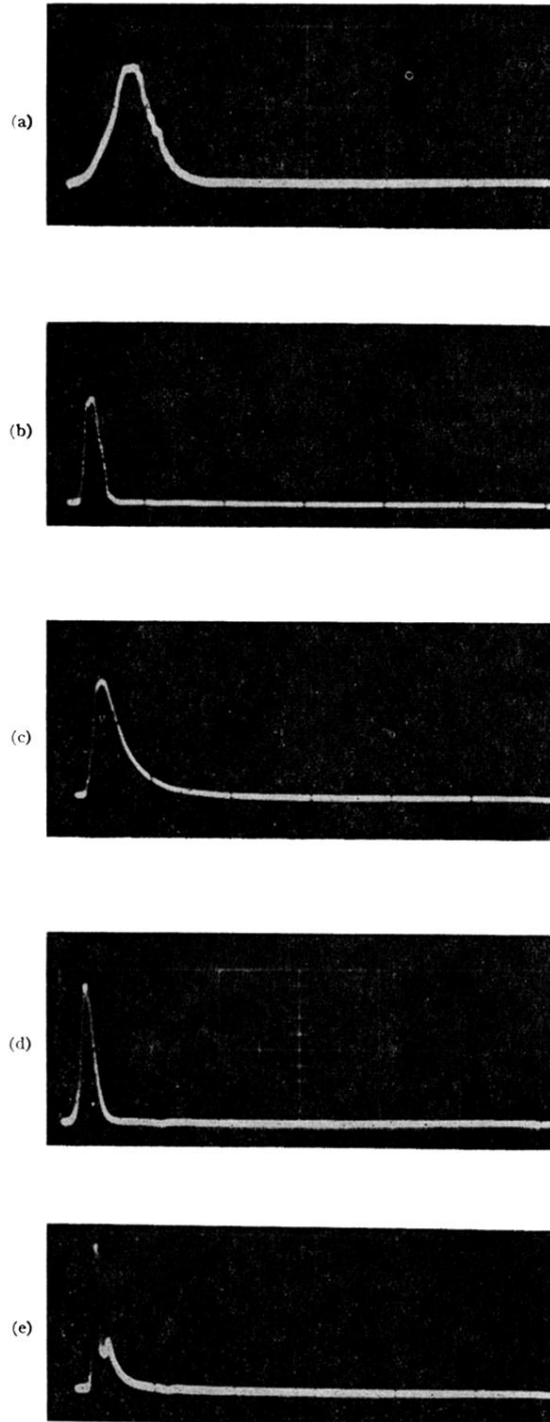


FIG. 5. Time-resolved stimulated Brillouin emission 20 nsec/div.; 1-GHz bandwidth. (a) Laser, ω_L ; (b) Brillouin at 180° in 12-cm cell of *n*-hexane with laser unfocused; (c) Brillouin at 90° in *n*-hexane; (d) Brillouin at 90° in nitrobenzene; (e) Brillouin at 90° in cyclohexane.